Constructed wetlands to solve agricultural drainage pollution in South Florida: development of an advanced simulation tool for design optimization

Joan Garcia[1,*], Alessandro Solimeno[2], Li Zhang[3], Darryl Marois[3,4] and William J. Mitsch[3]

[1]GEMMA-Group of Environmental Engineering and Microbiology, Department of Civil and Environmental Engineering, Technical University of Catalonia-BarcelonaTech, Spain

[2]Technical Institute of Canary Islands, Gran Canaria, Spain

[3]Everglades Wetland Research Park, Florida Gulf Coast University, Naples, FL USA

[4] Current address: U.S. Environmental Protection Agency, Pacific Coastal Ecology Branch, Newport, OR, USA

[*]Corresponding author. E-mail address: joan.garcia@upc.edu

Abstract

Eutrophication is a widespread global scale pollution problem. Agricultural areas are generally the main contributors to eutrophication, whereas sewage and industrial discharges, which usually receive some treatment prior to discharge, are a secondary source. This is mostly the case of the ultra-oligotrophic Florida Everglades, where natural water sources are often enriched by nutrients from large-scale industrial agricultural stormwater runoff. Remediation of these agricultural waters cannot be conducted with the usual environmental engineering solutions, and in this context ecological engineering approaches such as constructed wetlands are much more suitable. Moreover, these wetlands provide other ecosystem services such as carbon sequestration or habitat provisioning. In this paper we have implemented a mechanistic phosphorus model into a time-space-dependent mathematical simulation platform (COMSOL Multiphysics™) which has been calibrated with wetland mesocosm data. Subsequently we have evaluated different characteristics of constructed wetland physical elements such as internal walls and baffles, different types of inlets, parallel and series operation, and increase in hydraulic retention time (HRT) to study total phosphorus (TP) removal performance and to improve efficiency. Simulation results indicate that wetland mesocosm soils released dissolved organic phosphorus which was washed out together with the effluent, making very difficult to attain a concentration lower than a target of 10 μg TP L^{-1}, as required to protect the Everglades. Simulations showed that the design based on combination of the bottom inlet together with parallel operation extensively improves efficiency. Target TP concentrations can be achieved with this design together with an increase on 25% of hydraulic retention time. With this study we demonstrate the usefulness of the model for detailed designs, opening the door for its use in field scale applications.

Keywords: Agricultural runoff, modelling, storm treatment areas, STA, subtropical constructed wetland, treatment wetlands

1. Introduction

Constructed wetlands or treatment wetlands are nowadays a world widespread technology used for remediation of agricultural runoff. Drainage from agriculture practices is a type of non-point source pollution characterized by high and fluctuating flows in space and time, and relatively low concentrations of pollutants such as nutrients (in comparison to other wastes and wastewaters). Especially for these intrinsic properties, remediation of these agricultural waters cannot be conducted with the usual environmental engineering solutions, and in this context ecological engineering approaches such as constructed wetlands are much more suitable. Constructed wetlands provide large hydraulic retention times, and a number of differentiated compartments giving place to multiple microenvironments, where multitude of processes can interact among them for the benefit of water quality improvement (Dierberg et al., 2005; Kadlec, 2016).

Thus, there are numerous examples around the globe where this technology is being used at field scale as detailed by Land et al. (2016), being probably the known as storm treatment areas (STA) in South Florida the most extensively studied (Kadlec, 2016; Zamorano et al., 2018a, b). STAs are in fact surface-flow treatment wetlands which receive agricultural runoff from fields for protecting the great wetland Everglades. STAs were specially designed and constructed to remove phosphorus avoiding Everglades eutrophication, and with their more than 20,000 ha, they are presumably the largest constructed wetland system in the world (Chimney and Goforth, 2006). A number of reports as cited by Zambrano et al. (2018a) have demonstrated the superb capacity of STA for phosphorus removal. Nowadays, with all scientific and technical knowledge obtained in last years regarding operation, effluents with concentrations lower than 20 µg TP (total phosphorus) L^{-1} have been obtained (Mitsch et al., 2018). However, unfortunately, this is not enough to protect the ultra-oligotrophic Everglades ecosystems, for which stringent requirements lower than 10 µg TP L^{-1} must be achieved (Mitsch, 2016). This ultra-low TP concentrations are certainly difficult to achieve with current constructed wetland knowledge and practices because are in the concentration of what is assumed the background phosphorus level. In this regard, complex mechanistic models linked to simulation platforms can help to enable detailed engineering designs (for reaching effluent target concentrations), as it is usually done in other engineering branches like structural or mechanical engineering.

Sizing is a very important step during constructed wetland design, and this can be carried out through different approaches such as regressions from extended databases, areal loading rates of much more appropriated models such as the PkC* (Kadlec, 2016). However, these approaches models cannot assist in detailed designs including the number and location of inlets and outlets, internal walls and baffles, water depth, and much other elements that conform what is in the end an engineering project for its construction (Min and Wise, 2009; Persson, 2000, 2005; Persson et al., 1999). The complete design of a constructed wetland which has to achieve very stringent effluent TP requirements such as in south Florida has to be necessarily based on fine tuning of all their elements. Complex mechanistic models can allow for fine-tuning of constructed wetland elements, but they must be linked to multiphysics simulation platforms that allow space-dependent reactions to occur, as well as time-dependent reactions. The reason is that different constructed wetland detailed elements will be located in different point spaces. Also the quality of water, soil properties and biologic components will have space-dependent patterns. Mechanistic models have been long applied in wetland ecology using only time-dependent simulation platforms such as STELLA software (Marois and Mitsch, 2016). While these platforms allow into get insight into internal wetland functioning, they can't be used for detailed designs because lacking of space-dependent properties.

Therefore, in this study we have implemented a phosphorus mechanistic model within a space-time-dependent simulation platform (COMSOL Multiphysics™) which has been calibrated with mesocosms data. Subsequently we evaluated different characteristics of constructed wetlands physical elements (case studies) to study performance in TP removal and try to increase efficiency. With this study we demonstrate the usefulness of the model for detailed designs, opening the door for its use in field scale applications such as could be future STA designs.

2. Material and methods

2.1. Data for model

Data used for model were obtained from the study by Mitsch et al. (2015) in which 18 mesocosms surface flow constructed wetlands (6 m x 1 m x 1 m) planted with 6 different vegetation communities were monitored for a period of 3 years (from 2010 to 2013). These wetlands in West Palm, Florida, were filled with a local soil layer of 0.3 m from an adjacent treatment wetland (STA) and planted with different species of aquatic macrophytes. Note that this soil had moderate to high content of phosphorus (Mitsch et al. 2015, 2018). Water depth was maintained at 0.4 m above the soil thanks to a weir located at the outlet of each mesocosms. Each unit was fed with a flow of 156 L d^{-1} (2 pulses of 78 L per day, each in 30 min) giving as a result a nominal hydraulic retention time (HRT) and a hydraulic loading rate of 15.4 d and 2.6 cm d^{-1}, respectively. Influent flowrate at the moment of the pulses was 4.3E-5 m^3 s^{-1}, and therefore the sectional free water velocity 1.075 E-4 m s^{-1}, developing a strongly laminar flow (Re= 23.7, Supplementary materials). Water used for influent was pumped out from the effluent of a full scale surface flow constructed wetland (named STA-1W) fed with agricultural drainage, and therefore TP content was already quite low. Annual average of TP ranged from 20 to 30 µg L^{-1}, being approximately 60% particulate phosphorus (PP), 30% dissolved organic phosphorus (DOP) and 10% dissolved inorganic phosphorus (DIP) (Marois and Mitsch, 2016).

Effluent phosphorus data corresponding to averages from 3 mesocosms wetland replicas planted with cattail (*Typha domingensis*) were exclusively used in the present study. Data from the other mesocosms wetlands were not used because comparison between macrophytes was not the target of the research, we were more focused in physical elements. Macrophytes were extensively compared by Marois and Mitsch (2016). Wetlands planted with cattail were selected here because were those that showed the more stable TP removal efficiency. Only data from February 2012 to March 2013 were used for the purposes of the present study because a period of 1.5 years after starting operation was assumed to be by far wide enough to reach steady state conditions in terms of P removal. After this period plants were very well developed (approximately 1.5 kg m^{-2}). In addition to phosphorus species concentrations, other field data (solar radiation (PAR), air temperature, rainfall and potential evapotranspiration) necessary for the model were gathered from a meteorological station managed by the South Florida Water Management District located at 2.5 km from the place of mesocosms (https://www.sfwmd.gov/science-data/dbhydro). Water temperature was directly measured in the mesocosms (Mitsch et al., 2015).

2.2. Model domain and mesh

The whole domain was represented as a rectangle 6 m long and 0.7 m deep (Figure 1). Therefore, the model was two dimensional (2D). Three different domains were considered: free water (0.4 m deep), active soil (AS, 0.1 m deep) and deep soil (DS, 0.2 m deep). In water domain, water moves freely in contact with atmosphere, while in soil domains water flows through soil porous medium. Boundaries of right, left and bottom are impervious walls. AS was in direct contact with free water and it is assumed that in this part of the soil more intense reactions occurs. Influent water enters the domain on the top left side of the water and exits on the top left hand. It was assumed that the thickness of the inlet and the outlet was 0.03 m.

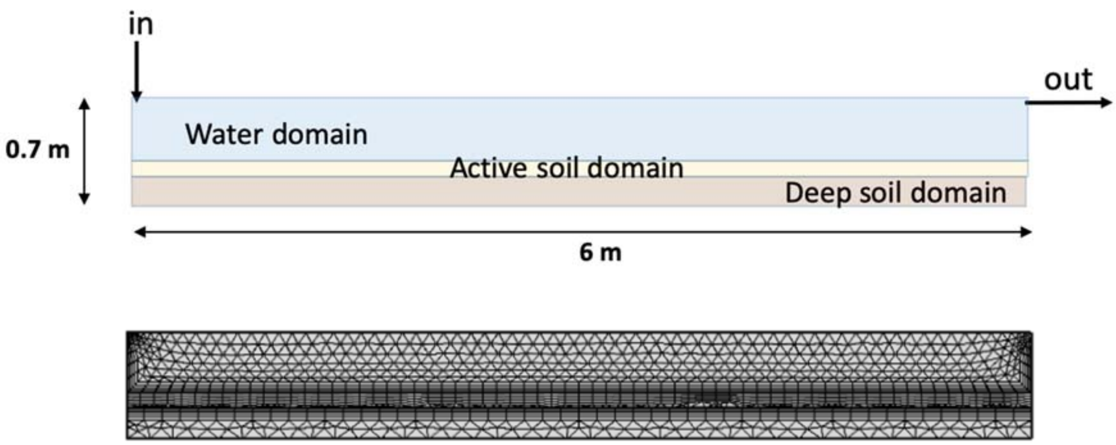

Figure 1. 2D schemes of mesocosm wetland (see Mitsch et al., 2015 for mesocosm details) with the three domains (water, active soil and deep soil) and location of inlet and outlet (above), and mesh of finite elements (below). Note mesh refinements in inlet, outlet and intermediate boundaries.

Mesh of finite elements where differential equations are solved is made up with 2213 triangular and quadrilateral elements, and with adaptative refinements in inlet, outlet and intermediate boundaries. Mesh was obtained from the automatic meshing tool of COMSOL Multiphysics^{TM}. Refinement was conducted to improve solution of the model in domain zones where it was expected to have more convergence instabilities.

2.3. Model equations

For the sake of an easier implementation and presentation, the model was split into four sub-models that were calibrated independently (similar to Samsó and García (2013a, b)): hydraulic, transport, plants and kinetic sub-models. Figure 2 shows the main processes and reactions occurring in the sub-models in the different domains. Model equations are presented in Appendix A. Note that default COMSOL Multiphysics^{TM} equations are not described in this paper, but can be found in Samsó and García (2013a).

Hydraulic sub-model was constructed with the Laminar flow interface of the COMSOL Multiphysics^{TM} which solves Navier-Stokes and continuity equations to compute velocity (**u**) and pressure (p) fields with in water domain for incompressible flow. For soil domain, this laminar flow interface of the COMSOL Multiphysics^{TM} enables porous media domains which are described with Brinkman equations in which porosity (ε) and permeability (κ) have to be defined. In the hydraulic sub-model water density (ρ) and dynamic viscosity (μ) change with water temperature according to the equations in Appendix A. Permeability was estimated from hydraulic conductivity, which was assumed constant (1E-4 m s^{-1}), and was a function of temperature because changed with water density and viscosity (Appendix A). Estimated permeability at 20 °C for example was 1.03E-11 m^2, which is in the order of magnitude of soils used in the mesocosms (Mitsch and Gosselink, 2015). A symmetry boundary condition was imposed into the air and water interface which prescribes no penetration and vanishing shear stresses. Also, a laminar flow boundary condition was imposed at the inlet to assume that water enters the domain with an already developed laminar flow.

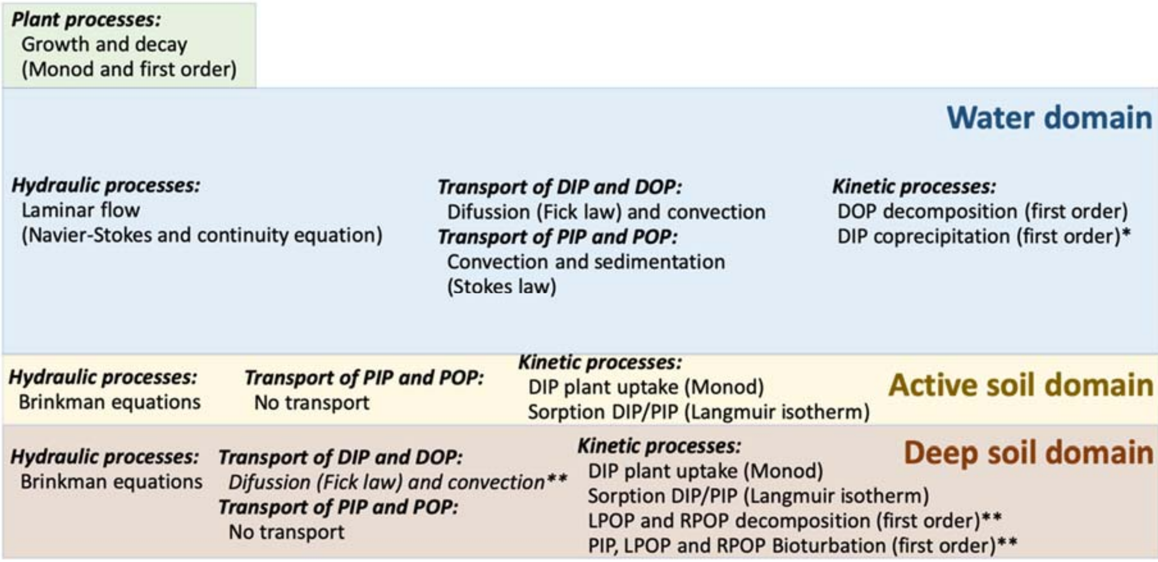

Figure 2. Main processes and reactions occurring in the three domains of the wetland mesocosms described in Mitsch et al., 2015, 2018. Note that we have used the scheme representation in Figure 1. Processes and reactions are detailed in Appendix A. *This reaction only takes place in free water. **These reactions also occur in active soil but were not written to avoid overlapping.

Transport sub-model was developed with the Transport of diluted species interface of the COMSOL Multiphysics™, which allows to calculate the concentration field of phosphorus species in water (which are therefore the dependent variables). Driving forces for transport of dissolved species (DIP and DOP) are diffusion through Fick's Law as well as convection coupled to water velocity field. In the case of particulate species (particulate inorganic phosphorus and particulate organic phosphorus, PIP and POP) diffusion was neglected. Also another specific condition imposed was lack movement for particulate species (**u** =0) in soil domains.

Plant sub-model included space-independent equations (from r_1 to r_5 in Appendix A) which were introduced into the COMSOL Multiphysics™ using the Global ODEs and DAEs interface. This means that the plants were the only element of the model assumed to be equally distributed in the wetland. Equations are essentially the same used by Marois and Mitsch (2016) and describe the variables (Appendix A): aboveground plant biomass (BM_{AG}) with Monod kinetics and the standing death plant biomass (BM_{SD}) with first order kinetics. In the model, belowground plant biomass (BM_{BG}) is computed as constantly 10% of BM_{AG}. Note that

BM_{AG} equation includes a different and more generalized logistic factor than that used by Marois and Mitsch (2016). Forcing functions for these variables are solar radiation (PAR) and air temperature (T_A). Variables related to phosphorus contained in the plant biomass (aboveground (P_{AG}), belowground (P_{BG}) and standing death (P_{SD})) are also calculated as space-independent variables with equations very similar to the ones used for plant biomass. Note that plant sub-model is not coupled with the hydraulic and transport models, thus in present model it is assumed that plants have no impact on water field velocities and HRT. This is an acceptable assumption in our case due to the very low water velocity (in the range of 1E-6 to 1E-4 m^3 s^{-1}). On the other hand, to represent the effect of plants in water movement it would had been necessary a 3D model.

Kinetic sub-model was introduced in the Transport of diluted species interface of the COMSOL Multiphysics™, which has a node that allows to add reactive terms to transport functions of each phosphorus species (from r_6 to r_{19} in Appendix A). As in plant sub-model, equations for reactive terms were essentially the same used by Marois and Mitsch (2016). The reader is referred to the original article to get in depth details of the kinetic model. Equations include the following variables: DIP, DOP, PIP, POP. Particulate phosphorus (PP) is calculated in the wetland and in effluent as the sum of PIP and POP. Total phosphorus (TP) is the sum of all particulate and dissolved species. In the model, POP only exits as itself in free water, because in soil is divided into four variables (depending on AS and DS): labile particulate organic phosphorus ($LPOP_{AS}$ and $LPOP_{DS}$) and recalcitrant particulate organic phosphorus ($RPOP_{AS}$ and $RPOP_{DS}$). Note that labile and recalcitrant POP were different variables in AS and DS (in contrast to the other phosphorus variables) because they are immobile, present in soil but not in water, and together with the fact that AS has much more interactions than DS. Reactions for DIP in free water include DOP decomposition, which is temperature dependent, and coprecipitation. DIP coprecipitation is the only reaction linked to a dissolved component that exclusively happens in water. Coprecipitation actually takes into account DIP occluded during calcium carbonate precipitation (Reddy, 2019). DOP in free water is only affected by its decomposition. DIP in the pore water of AS depends on the decomposition of DOP, plant uptake and sorption. Plant DIP uptake is essentially a function of plant growth, and is space-independent as plant growth is formulated in the model. Sorption is described with a first order kinetics in which the DIP equilibrium concentration is computed with the Langmuir isotherm. Last term of sorption equation is the isotherm (see Appendix A). Note that the soil particles can be a source or a sink of DIP depending on DIP equilibrium concentration. For that reason calibration of parameters related to sorption has been one of the most challenging parts of this work, since when the function takes negative values, strong nonlinear computational instabilities may appear and simulations can be suddenly stopped. DIP in pore water of DS is essentially described with the same equations as in AS. DOP in soil pore water is a function of temperature dependent processes of decomposition of labile POP an DOP.

PIP and POP depend on sedimentation in free water and the approach is simple and the same for both variables through Stokes law for spherical particles. It is assumed the same density for PIP and POP particles. PIP also is affected by coprecipitation. PIP in AS depends on sedimentation, sorption and bioturbation, which accounts for the mobilization of phosphorus from activity of aquatic organisms and it is described with a first kinetic reaction. Recalcitrant POP in AS depends on phosphorus coming from standing death biomass, belowground biomass death, its own decomposition and bioturbation. Labile POP in AS depends on POP sedimentation in free water, own decomposition and recalcitrant POP decomposition and bioturbation. Reactions for recalcitrant POP and labile POP in DS are very similar to those of AS.

Certainly, the mechanistic model does not include all the processes and reactions involved in the phosphorus cycle in wetlands, and so the model is, as always, a simplification of the reality. We have built up the model from the previous work by Marois and Mitsch (2016), in which more important processes were already selected and studied from an extensive literature review.

2.4. Calibration procedure

Simulations were run with a Dell OptiPlex 5050 computer with a processor Intel® Core™ i5-7600 (QC/6MB/4T/3.5GHz/65W). Hydraulic and transport sub-models were simultaneously calibrated using an indirect procedure since there weren't water velocity or pressure measurements available for mesocosms wetlands. This procedure consisted in assuming the injection of an unreactive dissolved tracer (at the same time of an influent discharge) and matching the estimated HRT with the nominal HRT. For the tracer, a hypothetical concentration of 25 μg L^{-1} was selected because measured influent TP ranged from 20 to 30 μg L^{-1}. A diffusion coefficient of 1.15E-10 m^2 s^{-1} was chosen, which was in the same order of magnitude than in Marois and Mitsch (2016). First, it was adjusted the width of the inlet to match the nominal HRT using the two daily influent discharges pattern. Then, with the adjusted width, a constant inflow was adjusted to match the nominal HRT. Note that a constant flowrate was assumed because with the two daily influent discharges pattern, simulations with the whole model lasted more than 15 hours, making unmanageable kinetic sub-model calibration. Once constant flow was already adjusted, the diffusion coefficient of the tracer was then adjusted to match the normalized variance (σ_{ϑ}^{2}) of the tracer response curve. Theory fundamentals and equations on estimations of HRT and σ_{ϑ}^{2} from tracer response curves can be found in García et al. (2004). For Hydraulic and Transport sub-models calibration evapotranspiration and rainfall were not taken into account. Constant 20 °C water temperature was assumed. Simulations were run with a time step of 0.5 h and were stopped at 800 h because in previous trials it was observed that at this time effluent tracer concentration was already very low. This 800 h simulation time is slightly lower than 3 times the nominal HRT (1,108 h). Simulations were run with a relative tolerance of 0.05. Initial values for water velocity, pressure and tracer concentration were set at 0.

The plant sub-model calibration was deliberated kept simple just adjusting parameters by visual comparison of measured and simulated data. We had only 3 measured values of plant biomass in the period from February 2012 to March 2013, and calibration intended to represent the general trend of these values. Initial values of the plant sub-model dependent variables are shown in Appendix A, and were taken from simulation results of Marois and Mitsch (2016) for November 2011, which was the start time for our simulations. Note that to improve accuracy, simulations of both plant as well as kinetic sub-models were started 3 months before the period of interest (February 2012 to March 2013). Thus, simulation time for the plant and kinetic sub-models was 477 days, with a time step of 17 days and relative tolerance of 0.005.

Kinetic sub-model calibration was the more complicated one and demanded a very intensive work due to high number of parameters involved (14). We essentially used the Parametric Sweep option of COMSOL Multiphysics™ which enables automatic loop simulations of combinations of different value parameters. In general we combined 5-6 parameters with 3-6 different values, giving place from 400 to 800 simulations which were run during 1 to 2 days. Calibration was conducted first matching effluent TP concentrations and subsequently refining for PP, DOP and DIP effluent concentrations. Adjustment between simulated and measured values was evaluated using averages and standard deviations of each relative error (RE) (Supplementary materials). A simulation was considered good when average and standard deviation RE of TP, DOP and PP was less than 10% and 40%, respectively. Note that in environmental simulation problems, an average RE lower than 20% is considered to be acceptable (Marois and Mitsch, 2016), independently of RE standard deviation. From the 400 to 800 launched simulations in each parametric sweep, those meeting RE criteria were graphically represented for final selection of calibrated parameters by visual comparison. In the case of DIP, RE were calculated as root relative square errors because high number of zeros in this variable (see Supplementary materials), and only a direct visual comparison was applied after other variables met RE criteria. Those parameters found to be more sensitive by Marois and Mitsch (2016) were first evaluated in parametric sweeps as a pragmatic way to start. Also note that influent PIP and POP concentrations were not measured and therefore were calculated from PP as 1/3 and 2/3, respectively, as usually is observed in the area (Marois and Mitsch, 2016). Initial values for phosphorus species in water were assumed, while values in sediments were taken from Marois and Mitsch (2016), except for DIP which was estimated from PIP using Langmuir term in variable R_{SORP} (term inside big brackets, see Appendix A and Supplementary materials).

For the calibration of the kinetic sub-model, evapotranspiration and precipitation were transformed into flow and inserted into the inlet as flowrates spread along the day, and therefore had effect on water field velocity and subsequently on HRT. However, impact of these two forcing functions was observed to be very low. Also we conducted several trials to introduce effect of evapotranspiration and precipitation on solutes concentration through a corrective term for concentration, but results were very confusing. Perhaps the effect of evapotranspiration and precipitation in concentration is negligible at the very low concentrations of the mesocosms wetlands. The evaporation was calculated multiplying the measured potential evapotranspiration by an evapotranspiration coefficient (K_{ET}) in order to consider the increased evapotranspiration in emergent aquatic vegetation.

In the present configuration of the model, hydraulic and plant sub-models can be run alone, while transport sub-model has to be connected to hydraulic sub-model, and kinetic sub-model depends on all the others.

2.5. Cases studies

A high number of different hypothetical design scenarios (case studies) of the mesocosms wetland were evaluated with the simulation model already calibrated. However, in this paper we present four scenarios which are representative examples and cover most of the variations evaluated: internal walls and baffles, bottom inlet, a combination of bottom inlet and parallel operation, and a combination bottom inlet, parallel operation and influent flow decrease (Figure 3). Note that a decrease in flow means an increase in HRT. The efficiency of each different case study was compared against results of the calibration original setup which were considered as “reference model”. In design with walls and baffle impervious walls were located 1.5 and 4.5 m from inlet, nailed onto soil and leave water to pass by a top 0.03 m free space. An impervious baffle was located at 3 m from inlet and assumed to hang on from a floating device. Baffle leaves water to pass by a bottom space of 0.03 m between baffle distal end and soil. Walls and baffle design intends to improve hydraulic behavior of mesocosms wetland. Bottom inlet design includes an inlet located just onto soil with a thickness of 0.03 m. This allows putting water immediately in contact with soil, where it is assumed that sorption retention reactions and also sedimentation will be improved. In bottom inlet and parallel operation design there would be 3 mesocosms wetlands 2 m long fed with 1/3 of the flow each. In this case HLR and HRT would be the same as in reference model, but not longitudinal velocity which would be globally 1/3 lower because decreasing flow while maintaining section surface. In bottom inlet, parallel operation and influent flow decrease in 75%, the HRT would be increased in 25% and the HLR decreased in 75%. In this case longitudinal velocity will be also lowered.

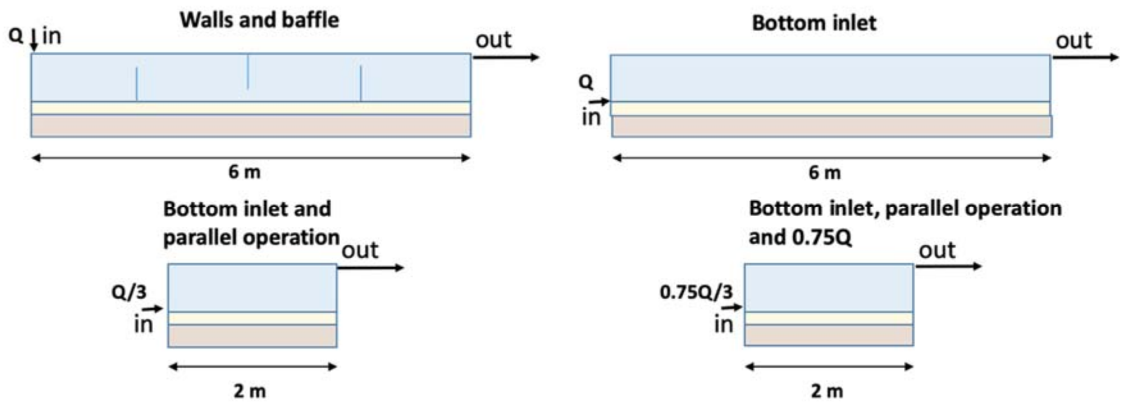

Figure 3. 2D schemes of design cases studies alternative to the calibrated original setup. In parallel operation designs only 1 wetland of the 3 parallel are represented.

For evaluation of cases studies TP concentration was taken as indicator. Simulations of case studies were run using the same data employed during calibration and therefore the only difference was design. In two case studies (walls and baffles, and lower inlet) it was necessary to make small changes in the mesh to avoid numerical instabilities.

3. Results and discussion

3.1. Calibration

Hydraulic and transport sub-models calibration started with adjustment of inlet width to match nominal HRT. Figure 4 shows the tracer curve response registered at mesocosms outlet for 3 different inlet widths. Analytically it can be seen that the point in the xth axis which divides the surface tracer curve response in 2 equal areas is the HRT (arrow in Figure 4 for 1.12 m inlet width). Inlet had to be adjusted to 1.12 m to match the nominal HRT, which is a 12%

higher than the real width of the mesocoms. This is due to relationship of the flowrate and assumed thickness of the inlet (0.03 m). The important point here was to match the HRT. In Supplementary materials there is a movie of the travel of tracer from inlet to outlet.

With the inlet width calibrated, then we adjusted a constant flow to attain the nominal HRT. As explained in the Methods section, this was necessary to make the model manageable. The adjusted flow was 1.8E-6 $m^3\ s^{-1}$, which in fact matches perfectly the flow obtained if the 156 L would had been spread all day round. Diffusion coefficient for tracer was subsequently calibrated as 3.472E-9 $m^2\ s^{-1}$ because it was the one that gave more similar σ_ϑ^2 to the tracer curve response of the initial calibration of the inlet width (1.1E3 vs. 9.6E3, being the last number for initial calibration). Calibrated diffusion coefficient is more similar to experimentally measured values for orthophosphates of around 1.0E-8 (Hatfield et al., 1966), which contrasts with the initial value assumed in the range to that from Marois and Mitsch (2016). Note that different values of the diffusion coefficient did not give much differences in σ_ϑ^2, suggesting that in mesocosms wetlands, convection transport processes were of much more importance than diffusion. Note that calibrated value of diffusion coefficient was used for all dissolved P species ($K_{DI,\ DIP}$ and $K_{DI,DOP}$).

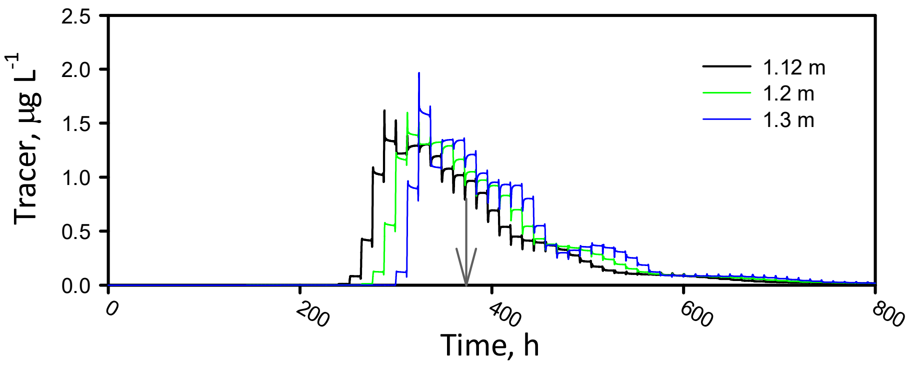

Figure 4. Tracer curve responses at outlet of mesocosms for 3 different inlet widths. With a 1.12 m width nominal HRT was matched. The arrow points mean HRT for 1.12 m curve, which is the point in the xth axis which divides the surface tracer curve response in 2 equal areas. Note the stepwise pattern of curves which is linked to influent discontinuous discharge strategy.

Figure 4 shows the water velocity field and Figure 5 a velocity profile in the middle length (3 m) and near outlet (5.9 m) of the mesocosms wetland. Water influent enters the water on the top left and flows slowly towards the outlet on the top right. In the yth direction there is a decrease in the velocity from the top of the water in contact with air to the water near the soil. This is the reason why most of tracer travels through the top of free water as shown in the movie of Supplementary materials. Also the relative small amount of tracer moving near the bottom of free water is linked to the long tails of tracer response curves in Figure 4. When water approaches outlet, there is an increase in upper velocity (Figure 6). In the soil, pore water movement is negligible of several orders of magnitude lower than in the free water (1.0E-9 m s^{-1}). Simulated average velocity in free water at a line transect in the mid length of the wetland is 2.76E-6 m s^{-1}, which is clearly lower than the estimated nominal velocity during discharges in the real operation (1.075 E-4 m s^{-1}). This behavior is of course a simplification of the model because assuming a constant flow, however the impact of this assumption on simulation results was reduced thanks to matching HRT and σ_{ϑ}^2.

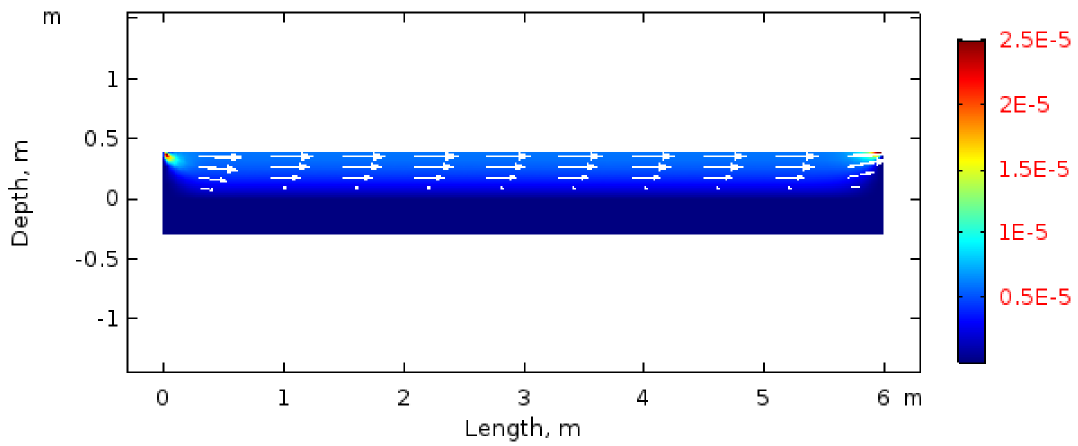

Figure 5. 2D section of wetland mesocosms water velocity field with an adjusted constant flow of 1.8E-6 m^3 s^{-1}. Length of the wetland (6 m) is represented in the xth axis, while depth (0.4 m for free water domain + 0.3 m for soil domains) in the yth axis. Color bar in the right represents water velocity in m s^{-1}. Arrows indicate flow direction and their size is proportional to velocity.

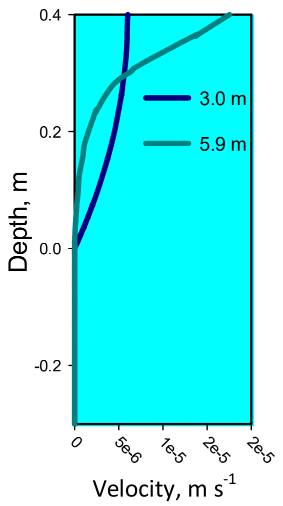

Figure 6. Velocity profile at cut vertical lines located at 3 m and 5.9 m of the length of the mesocosms wetland. Blue zone represents water and brown zone soil. Velocity in soil domain is negligible. Profile at 5.9 corresponds to right wall of mesocosms wetland where outlet is located.

Figure 7 shows how the model adequately matches field measured aboveground plant biomass (standing death plus alive biomass). Note that the plant sub-model was described with global space-independent reactions and therefore it was assumed a constant distribution for plant density. In Figure 7 it can be seen an increase in the biomass in the warmest period of the year and a relative constant behavior for the rest. This contrasts with the results of the paper by Marois and Mitsch (2016), in which a conspicuous decrease in aboveground biomass was observed in colder periods. There is no apparent clear reason for this discrepancy between models, but for cattail and in south Florida, it seems more logical to have an almost constant biomass or little decrease in autumn and winter (Mitsch and Gosselink, 2015).

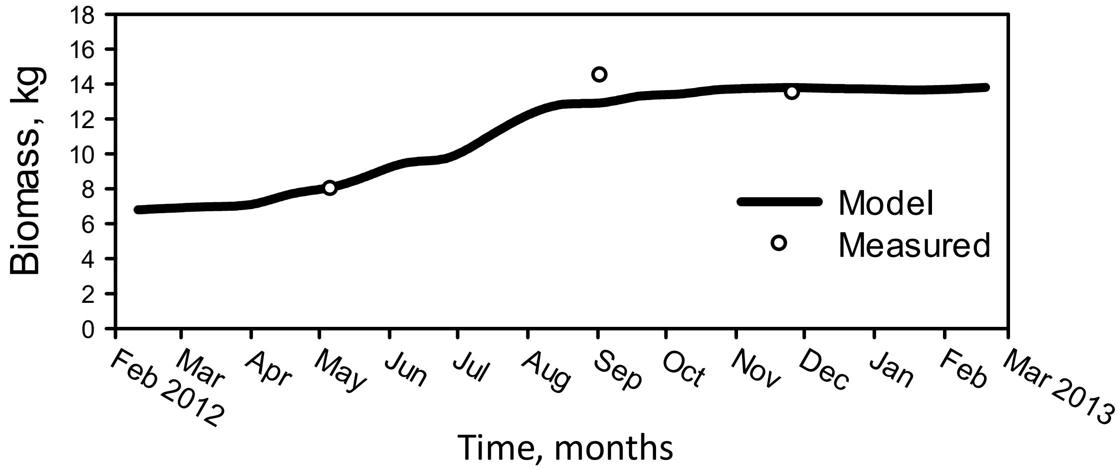

Figure 7. Simulated changes during calibration and measured total aboveground biomass in the mesocosms wetland (calibration).

Figure 8 show adjustment between model and field measured values of P species. RE were less than 10% (-2.7% for DOP, 8.2% for PP and -6.6% for TP), except for DIP which was 160% due to large number of very low values. Thus, results of calibration were considered of quite high quality with lower RE than those in the study by Marois and Mitsch (2016). Simulations and field data indicate that most of effluent TP was as DOP (approximately 60%), followed by PP (35%) and finally DIP (5%).

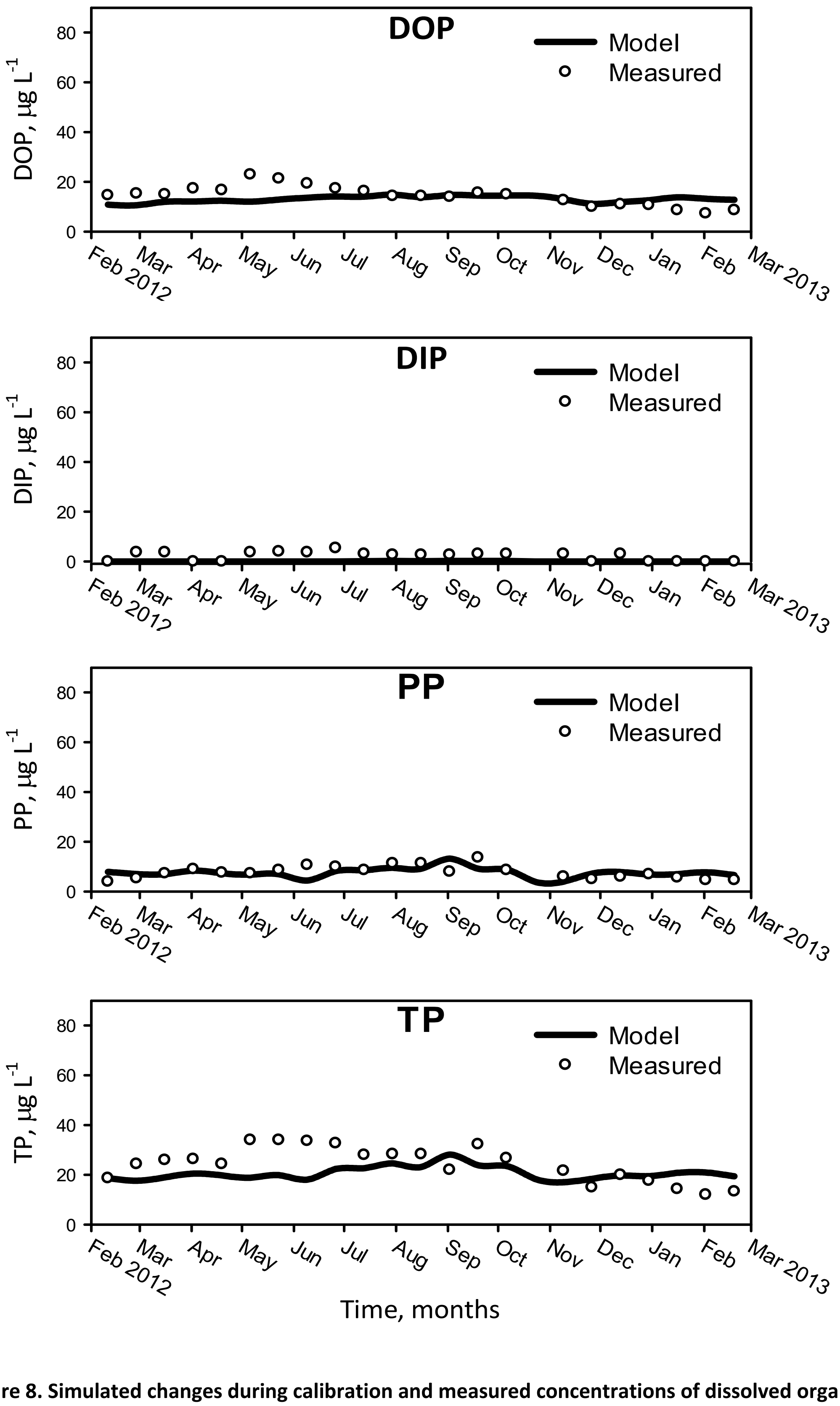

Figure 8. Simulated changes during calibration and measured concentrations of dissolved organic phosphorus (DOP), dissolved inorganic phosphorus (DIP), particulate phosphorus (PP) and total phosphorus (TP) in the mesocosms wetland.

In addition to RE evaluation, results of the calibration of the complete model were qualitatively verified analyzing internal behavior of phosphorus dependent variables. Average phosphorus in soil matched very well to two field measurements available (Figure 9). Globally, phosphorus in soil seemed to have a slight time decreasing trend, and in particular organic phosphorus species (DOP, LPOP and RPOP) were responsible for the pattern (Supplementary materials, Table S1). This is not in agreement with observations in field scale STA in South Florida, where influent phosphorus loadings increased the relative proportion of all phosphorus species in soil (Reddy, 2019). This difference could be due to the fact that mesocosms wetlands were pretty young in terms of operation in comparison to STA, and part of the soils phosphorus went to plants pools. In STA plant pools probably reached their maximum many years ago because they have been in operation for more than 20 years, and therefore phosphorus necessarily has to accumulate in soil. In Table S1 it can be seen that a large proportion of phosphorus in soil was in organic form as it is observed in field scale STA (Reddy, 2019).

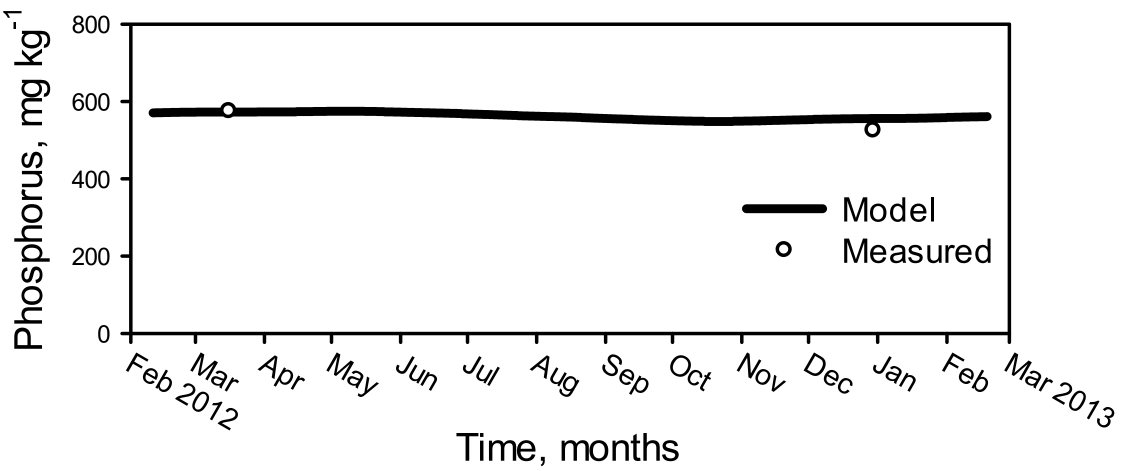

Figure 9. Average simulated changes and measured concentrations of phosphorus per kg of soil. Phosphorus calculated as sum of all species in soil (DIP+DOP+PIP+LPOP+RPOP). Average calculated as a surface average including active and deep soil (see Supplementary material, Table S1).

There were very strong gradients between soil and water in all phosphorus species as demonstrated in concentration profiles (Figure 10). Profiles for the same phosphorus species were in general quite similar in different places (cut lines) of the mesocosms wetland, so Figure 10 is representative of the whole wetland. This spatial phosphorus content homogeneity has not been found in field scale STA (Reddy, 2019), and again could be related to age of wetland mesocosms evaluated in the paper and also their small size. It is worth noting the increased concentration of DOP in few mg L^{-1} in free water just above soil in comparison to the other species (red arrow in Figure 10). This result suggests that soil is exporting DOP to free water and it has a strong influence on final effluent quality. Increased water velocity of the water near the outlet washes up DOP from bottom as can be seen in the little graph in Figure 10 comparing concentration profiles at 3.0 and 5.9 m, and in the 2D section of Figure 11 (green arrow). In fact in Figure 11 it can be seen that increased concentration appears like a blue light "cloud" onto the top of the soil in all entire length of wetland mesocosms. Figure S1 in Supplementary materials give additional insight into this pattern. Altogether these results explain why DOP is the predominant species in effluent mesocosms wetland. The model represents shows P mining from deep soil to active soil as indicated by the increase in organic particulate phosphorus concentration (LPOP and RPOP) in the active soil (Figure 10). This is a property observed in wetlands with big emergent aquatic vegetation with large and deep root systems (Zamorano et al., 2018b).

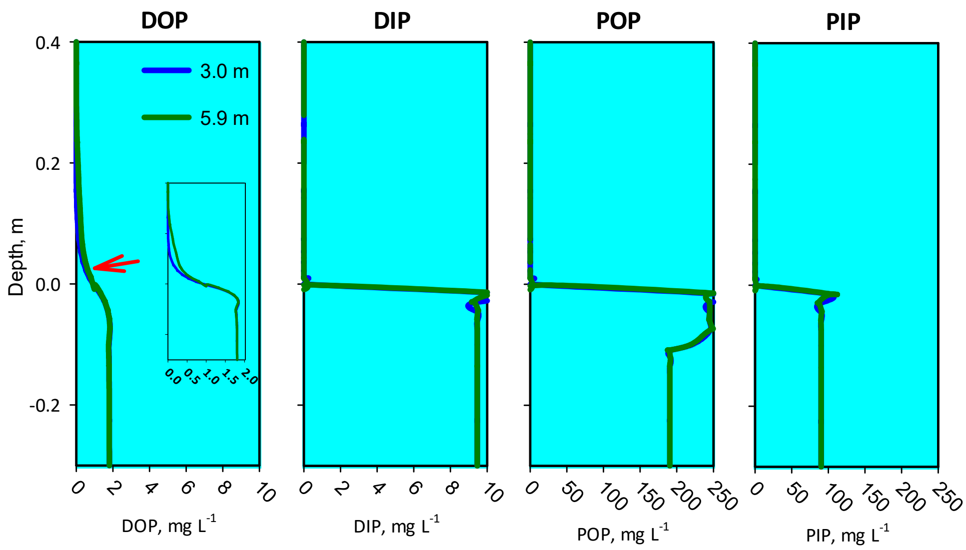

Figure 10. Phosphorus species profiles at cut vertical lines located at 3.0 and 5.9 m of the length of the mesocosms wetland from simulated data of September 2012 as representative example (in all other simulation times had same patterns). Blue zone represents water and brown zone soil. Note that concentration scales (xth axis) are different. Profile at 5.9 corresponds to right wall of mesocosms wetland where outlet is located. Inner little graph in DOP is the same graph with increased resolution in the xth axis (from 0 to 2 mg L^{-1}). Red arrow points out high DOP concentration in water just above soil. POP in sediment is in fact sum of labile and recalcitrant organic phosphorus (LPOP+RPOP).

Finally, we have to point out that in the model by Marois and Mitsch (2016) a sensitivity analysis was conducted and we have used their results for calibrating our model. However, we haven't conducted a specific sensitivity analysis to identify which input parameters influence the uncertainty of predictions as in the work by Flores-Alsina et al. (2009). This is a future work necessary to be done specially taking into account the great number of parameters included in our model.

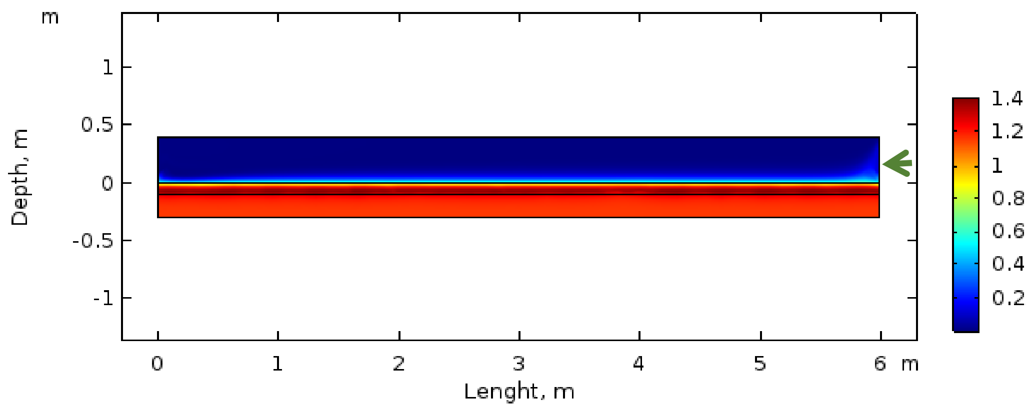

Figure 11. 2D section of wetland mesocosms DOP concentration from simulated data of September 2012 as representative example (in all other simulation times had same patterns). Length of the wetland (6 m) is represented in the xth axis, while depth (0.4 m for free water domain + 0.3 m for soil domains) in the yth axis. Color bar in the right represents concentration in mg L^{-1}. Green arrow points out how DOP "cloud" on the top of soil is washed out near outlet.

3.2. Case studies

Simulated data were not validated against real systems because simulations were conducted in fact over hypothetical scenarios. The walls and baffle scenario had the worse result of alternative designs, with effluent TP concentration even higher than in reference model (Figure 12). In this scenario it was presumed than an improvement in hydraulic behavior making bulk water to pass through most volume of wetland would increase efficiency. Bottom DOP wash up was increased with this design, in particular in the baffle influence zone (Figure S2). Bottom inlet design had slightly better results than reference model in warm season which were linked to higher removal of DIP and in turn in PIP due to increasing rates of sorption. Note that bottom inlet had a very local influence on water field velocity not having an appreciable effect on increasing DOP wash out (Figure S3). When parallel operation was applied to bottom design there was an amazing effect on effluent TP concentration which was much lower than in reference model, and this rise in efficiency was clearly linked to a lower wash out due to decreasing water horizontal velocity (compare Figures 13 and 5). In warm season TP removal was lower than other periods of the year. Only when flow was decreased in 75%, together with parallel operation and bottom inlet the effluent TP concentrations met much of time the target requirement. Decreasing flow in other words means increase the surface of the wetland.

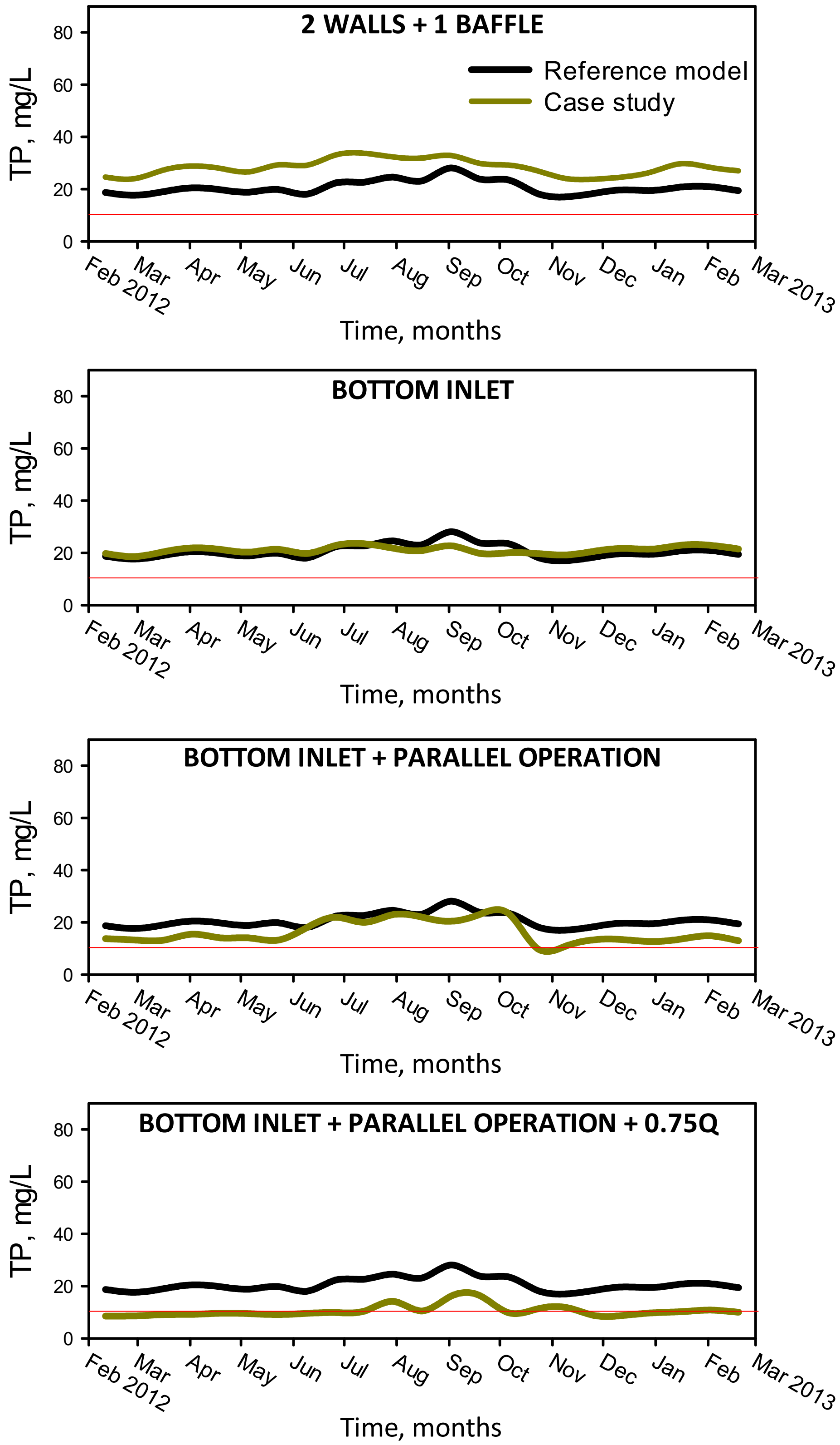

Figure 12. Case studies simulation results using effluent total phosphorus (TP) as indicator. "Reference model" are the results of the original calibration and used for comparison of each case study result. Also the 10 µg TP L^{-1} target requirement is shown (red line).

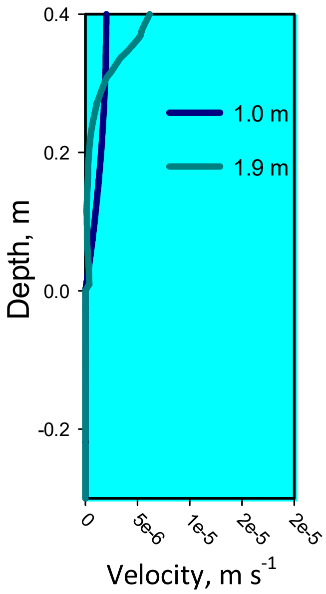

Figure 13. Velocity profile at cut vertical lines located at 1 m and 1.9 m of the length of the mesocosms wetland in the case study with bottom inlet and parallel operation. Blue zone represents water and brown zone soil. Profile at 1.9 corresponds to right wall of mesocosms wetland where outlet is located.

3.3. Implications for field scale systems

Certainly, results of case studies evaluated in this paper can’t be straightforward extrapolated for the design of field scale constructed wetlands for P removal. There are limitations concerning the representativity of the mesocosms wetlands, their physical geometry and the construction of the model. First, the model was developed from mesocosm wetland data that didn’t have intrinsic characteristics usually observed in field scale systems such as space diversity patterns in vegetation and varied flow patterns (Mitsch et al., 2015, 2018). Second, and very important, mesocosms wetlands are geometrically distorted prototypes with exaggerated vertical dimensions (depth) in relation to horizontal dimensions. Also, kinematic (water velocities) and dynamic (relation among forces) hydraulic similarities between wetland mesocosms and field scale wetlands will sure be different. Finally, there are several processes in the mechanistic model that can be improved with a better mathematical formulation. In particular phosphorus sedimentation processes can be solved with a more rational approach. Also, the number of phosphorus forms in sediment can be redefined depending on their reactivity, as well as the layers in the soil of wetlands.

However, despite all these drawbacks, results strongly stress the importance on detailed construction engineering aspects such as inlets/outlets and parallel/series operation, as already pointed out in field reference articles 20 years ago by Persson and coworkers (Persson et al., 1999, Persson, 2000). The practical implementation of the model puts into evidence the relevance of HRT, and therefore the surface necessary for the wetland. With no doubt a new field scale wetland can be sized with general models such as the PkC* model if parameters are derived from extensive data sets derived from previous experience on constructed wetlands already functioning (Kadlec, 2016). But to attain such a low concentration of 10 μg TP L^{-1} as in Florida STA, detailed design (fine tuning) with powerful simulation tools is highly recommendable if not obligatory. The model used here could be calibrated and validated with data from field scale systems, and used in a similar way to study different options as we did in the present study. With enough computer power, hundreds of combinations of different design options can be simulated and tested for the benefit of a reliable design.

The main theoretical input of the model is the importance of soil in constructed wetlands used for P removal in relation to the strong gradients between water and soil. This is already a well-known experimental property, and in fact, in field scale practical applications in Florida native rich phosphorus soil was removed down to the limestone bedrock or covered with limestone to reduce P soil release (Zamorano et al., 2018a, b). In our study, mesocoms wetlands had native soil with moderately high phosphorus and wetlands outflow phosphorus concentrations exceeded inflow concentrations during the first 1.5 years (Mitsch et al., 2015). Even after these 1.5 years, simulation results indicate that DOP soil release was still occurring and it is not known at what time this pattern could stop. However, it seems that it might take several years to stop and this support the fact that mesocosms experimental studies had to be enlarged as claimed by Mitsch et al. (2015, 2018). In our particular case, slow degradation rate of LPOP is the reason behind DOP soil release, and only will stop in the time point where rates of formation and degradation of LPOP will equilibrate. Altogether this information points out the importance to study soil properties carefully before any field scale wetland construction. Also, these results remark the great value of mechanistic models applied in time-space-dependent mathematical simulation platforms to understand processes in wetlands.

Another recommendation drawn from present study for field scale systems is that varied flows into the constructed wetlands must be avoided in the possible measure. Nowadays, STA in Florida receive varied flows depending on rainfall episodes and there is experimental evidence on their negative impact on performance during peak flows (Zamorano et al., 2018). In our simulation study it is clear that parallel operation had positive effect on performance thanks to decreased water horizontal velocity. In that case, a decrease in the water velocity linked to parallel operation had impact on reducing DOP wash out.

4. Conclusions

In this study we implemented a complex mechanistic model into a space-time-dependent simulation platform to study the behavior of the mesocosms constructed wetlands and their performances under different design scenarios. The modelling works clearly indicated that wetland soil was releasing dissolved organic phosphorus which was washed out together with the effluent, making very difficult to attain a concentration lower than a target of 10 µg TP L^{-1} as required to protect the ultra-oligotrophic Everglades in Florida. Different design scenarios were evaluated for improving efficiency of the TP reduction, and it was showed that combination of a bottom inlet together with parallel operation and an increase of 25% of hydraulic retention time could allow to reach target TP concentration.

With this study we demonstrate the usefulness of the model for detailed designs, opening the door for its use in field scale applications such as could be future STA designs. Future works include a better mathematical formulation for sedimentation processes, and redefining the number of phosphorus forms in sediment and the layers in the soil of wetlands and calibration and validation with data from field scale systems. Also, a sensitivity analysis has to be done to identify uncertainty in predictions.

Akcnowledgements

This work has been possible thanks to US Fulbright Program which under Salvador the Madariaga Program (Spanish Department of Education, Culture and Sports) that gave support to Joan García as visiting scholar during 6 months to the Everglades Wetland Research Park, Florida Gulf Coast University, Naples, FL, USA. Joan García also thanks his university (Technical University of Catalonia-BarcelonaTech, UPC) for giving a Sabbatical permission.

References

Chimney, M.J. and Goforth, G. (2006), History and description of the Everglades Nutrient Removal Project, a subtropical constructed wetland in south Florida (USA). Ecol. Eng., 27, 268-278.

Dierberg F.E., Juston J.J., DeBusk T.A., Pietro K. and Gu B. (2005). Relationship between hydraulic efficiency and phosphorus removal in a submerged aquatic vegetation-dominated treatment wetland. Ecological Engineering 25(1), 9-23.

García, J., Chiva, J., Aguirre, P., Álvarez, E., Sierra, J.P. and Mujeriego, R. (2004). Hydraulic behaviour of horizontal subsurface flow constructed wetlands with different aspect ratio and granular medium size. Ecological Engineering 23, 177-187.

Flores-Alsina, X., Rodriguez-Roda, I., Sin, G. and Gernaey, K.V. (2009). Uncertainty and sensitivity analysis of control strategies using the benchmark simulation model No1 (BSM1). Water Sci. Technol. 59(3): 491-499. doi: 10.2166/wst.2009.871.

Hatfield, J.D., Edwards, O.W., and Dunn, R.L. (1966). Diffusion coefficients of aqueous solutions of ammonium and potassium orthophosphates at 25°. J. Phys. Chem., 70 (8), 2555–2561. DOI: 10.1021/j100880a022.

Kadlec, R.H. (2016). Large constructed wetlands for phosphorus control: A Review. Water 8, 243. Doi:10.3390/w8060243.

Land, M., Granéli, W., Grimvall, A., Hoffmann, C.C., Mitsch, W.J., Tonderski, K.S., Verhoeven, J.T.A. (2016) How effective are created or restored freshwater wetlands for nitrogen and phosphorus removal? A systematic review. Environmental Evidence 5, 9.

Marois, D.E. and Mitsch, W.J. (2016). Modeling phosphorus retention at low concentrations in Florida Everglades mesocosms. Ecological Modelling 319, 42-62.

Min J.-H., Wise W.R. (2009). Simulating short-circuiting flow in a constructed wetland: The implications of bathymetry and vegetation effects. Hydrological Processes 23(6), 830-841.

Mitsch W.J. (2016). Editorial: Restoring the greater Florida Everglades, once and for all. Ecological Engineering 93, A1-A3.

Mitsch, W.J. and Gosselink, J.G. (2015). *Wetlands, 5th ed.*, John Wiley & Sons, Inc., New York

Mitsch, W.J., Marois, D., Zhang, L. and Song, K. (2015). Protecting the Florida Everglades wetlands with wetlands: Can stormwater phosphorus be reduced to oligotrophic conditions? Ecological Engineering 80, 8-19.

Mitsch, W.J., Marois, D., Zhang, L. and Song, K. (2018). Editorial: Protecting water quality of the Florida Everglades: Sustainably achieving low phosphorus concentrations with wetlands. Ecological Engineering 116, 174-177.

NAVFAC (1986). Soil Mechanics. Design Manual 7.01. Naval Facilities Engineering Command, Alexandria, USA.

Persson, J. (2000). The hydraulic performance of ponds of various layouts. Urban Water 2, 243-250.

Persson J. (2005). The use of design elements in wetlands. Nordic Hydrology 36(2), 113-120.

Persson J., Somes N.L.G. and Wong T.H.F. (1999). Hydraulics efficiency of constructed wetlands and ponds. Water Science and Technology 40(3), 291-300.

Reddy, K.R. (2019). Phosphorus biogeochemistry in wetlands: inside the black box. In: Book of abstracts of the 8th International Symposium on Wetland Pollutant (17 – 21 June, 2019, Aarhus University, Denmark). Edited by: Arias, C.A., Ramírez-Vargas, C.A, Peñacoba-Antona, L. and Brix, H. p. 26.

Samsó, R. and García, J. (2013a). BIO_PORE, a mathematical model to simulate biofilm growth and water quality improvement in porous media: application and calibration for constructed wetlands. Ecological Engineering 54, 116-127.

Samsó, R. and García, J. (2013b). Bacteria distribution and dynamics in constructed wetlands based on modeling results. Science of the Total Environment 461-462, 430-440.

Zamorano M.F., Piccone T. and Chimney M.J. (2018a). Effects of short-duration hydraulic pulses on the treatment performance of a periphyton-based treatment wetland. Ecological Engineering 111, 69-77.

Zamorano, M.F., Bhomiab, R.K., Chimney, M.J. and Ivanoff, D. (2018b). Spatiotemporal changes in soil phosphorus characteristics in a submerged aquatic vegetation-dominated treatment wetland. Journal of Environmental Management 228, 363-372.